P-ISSN 2586-9000
E-ISSN 2586-9027
Homepage : https://tci-thaijo.org/index.php/SciTechAsia
Science & Technology Asia
Vol. 26 No.4 October - December 2021
Page: [198-208]
Original research article

Influence of Slip of a Jeffrey Fluid Flow controlled by Peristaltic Transport with Nanoparticles in an Inclined Tube

Nemani Subadra[1], Mantripragada Ananatasatya Srinivas[2], Sunil Dutt Purohit[3,*], Sushila[4]

[1]*Department of Mathematics, Geethanjali College of Engineering and Technology, Telangana 501301, India*
[2]*Department of Mathematics, Jawaharlal Nehru Technological University, Kukatpally, Hyderabad, Telangana 500085, India*
[3]*Department of HEAS (Mathematics), Rajasthan Technical University, Kota 324010, India*
[4]*Department of Physics, Vivekananda Global University, Jaipur, Rajasthan 303012, India*

Received 26 August 2021; Received in revised form 15 November 2021
Accepted 04 December 2021; Available online 30 December 2021

ABSTRACT

The present investigation mainly focused on the effect of slip on a Jefferey fluid flow with nanoparticles in an inclined tube. Homotopy perturbation method is used to find the expressions for temperature and concentration. Analytical expressions for axial velocity, pressure drop, heat and mass transfer phenomena were calculated. The nature of these variables was interpreted by using the graphs for various pertinent parameters. Stream line patters were depicted at the end. The flow velocity can be controlled by increasing/decreasing the parameters $N_b, N_t, G_r, B_r, \lambda_1$.

Keywords: Homotopy perturbation method; Jeffery fluid; Prone tube; Slip effect

1. Introduction

Many researchers have recently focused on non-Newtonian fluid models due to their ubiquitous use in engineering and industry to investigate the thermo-physical characteristics of various parameters to improve the heat transmission properties of these liquids. Several investigators researched diverse non-Newtonian model fluids, Jeffrey fluid being one of them, for the exploration of various rheological characteristics. Shapiro et al., [16], Chu and Fang [2], Maruthi Prasad and Radhakrishnamacharya, [9], Prasad et al. [14], Subadra et al. [11].

Researchers are paying close attention to nanotechnology these days because of its applicability in health and industrial domains. S.U.S. Choi [15] was a pioneer in the field of nanotechnology

***Corresponding author:** sunil_a_purohit@yahoo.com **doi:** 10.14456/scitechasia.2021.80

research. Eastman et al. [3] shown that by adding nanoparticles to the base fluids, the thermal conductivity of the base fluids may be increased by 60%. Many other researchers have also worked in this topic. Significant contributions to this field of study have been made by Prasad et al. [8], Ellahi [4], Agarwal et al. [1], Jamshed et al. [7], Subadra et al. [8] and W. Jamshed et al. [17].

The majority of the researchers conducted their investigation with no slip boundary conditions at the vessel walls. Blood vessel walls, on the other hand, may be mobile, flexible, and porous in nature. Peristaltic transfer in a slip flow was studied by Chu and Fang [2]. Naby and Shamy investigated the effects of slip on the peristaltic transport of a power-law fluid via an inclined tube [12]. Slip effects on peristaltic transport in an inclined channel with mass transfer and chemical reaction were investigated by Hayat et al. [5]. Prasad et al. [8] investigated research on effect of slip of nanofluid in an inclined tube.

This work examines the peristaltic motion of nanoparticles submerged in Jeffery fluid in a conduit, as well as the impacts of heat and mass transmission. For axial velocity, pressure drop, frictional force, heat, and mass transfer effects, analytical formulas have been computed and graphed. The patterns of stream lines and trapped bolus have been illustrated.

Nomenclature

a^* Radius of uniform cross section,
b^* Wave amplitude,
c^* Speed of the wave,
N_b Brownian Motion Parameter,
N_t Thermophoresis Parameter,
p Pressure in wave,
P Pressure in fixed frame,
B_r Local Nanoparticle Grashof Number,
G_r Local Temperature Grashof Number,
F Frictional Force,
r Radial coordinate,
t Time,
k Permeability Constant,
U,W Velocity components in the laboratory frame,
u,w Velocity components in the wave frame.

Greek Symbols

μ Coefficient of viscosity,
λ^* Wavelength,
τ Cauchy stress tensor,
λ_1 Ratio of relaxation to retardation times,
λ_2 Retardation time,
γ Shear rate,
θ_1 Temperature,
σ_1 Concentration,
α Inclined angle.

2. Mathematical Formulation

In an inclined tube, a two-dimensional peristaltic propulsion of an incompressible Jeffrey model with permeable walls is investigated.

By using the cylindrical polar coordinate system (R,θ,Z), the fluid motion is caused by a sinusoidal wave train is

$$\mathrm{R} = H(z,t) = a^* + b^* \sin\frac{2\pi}{\lambda^*}(Z - c^* t). \tag{2.1}$$

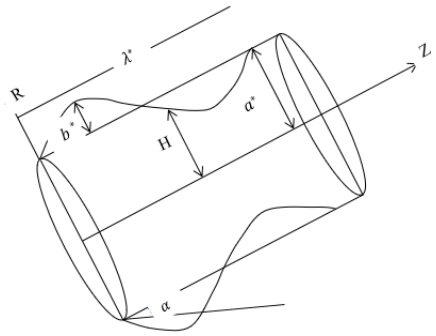

Fig.1. Geometry of the Problem.

For the Jeffrey model, the equation regulating the additional stress tensor τ is

$$\tau = \frac{\mu}{1+\lambda_1}\left(\frac{dY}{dt} + \lambda_2 \frac{d^2Y}{dt^2}\right). \tag{2.2}$$

To shift to wave frame, perform the transformations listed below.

$$z = Z - c^* t, r = R, \theta = \theta, w = W - c^*, u = U. \tag{2.3}$$

The equations of the Jeffery fluid flow (Nadeem et al. [13]) with nanoparticles may be obtained by using non-dimensionalization plus lubrication theory approximations:

$$\frac{\partial p}{\partial r} = 0, \tag{2.4}$$

$$\frac{1}{1+\lambda_1}\frac{1}{r}\frac{\partial}{\partial r}\left(r\frac{\partial w}{\partial r}\right) = -\frac{\partial p}{\partial z} + G_r\theta_1 + B_r\sigma_1 + \frac{\sin\alpha}{F}, \tag{2.5}$$

$$0 = \frac{1}{r}\frac{\partial}{\partial r}\left(r\frac{\partial \theta_1}{\partial r}\right) + N_b\frac{\partial \sigma_1}{\partial r}\frac{\partial \theta_1}{\partial r} + N_t\left(\frac{\partial \theta_1}{\partial r}\right), \tag{2.6}$$

$$0 = \frac{1}{r}\frac{\partial}{\partial r}\left(r\frac{\partial \sigma_1}{\partial r}\right) + \left(\frac{N_t}{N_b}\right)\frac{1}{r}\frac{\partial}{\partial r}\left(r\frac{\partial \theta_1}{\partial r}\right), \tag{2.7}$$

The following are the boundary conditions:

$$\frac{\partial w}{\partial r} = 0, \frac{\partial \theta_1}{\partial r} = 0 \text{ and } \frac{\partial \sigma_1}{\partial r} = 0 \text{ at } r = 0, \tag{2.8}$$

$$w = -k\frac{\partial w}{\partial r} = 0, \theta_1 = 0, \sigma_1 = 0 \text{ at } r = h. \tag{2.9}$$

3. Problem-Solving Approach

He's [6] HPM is used to get approximate solutions for θ_1 and σ_1 in Eq. (2.6) and Eq. (2.7). The expressions for θ_1 and σ_1 are obtained by applying boundary conditions and assuming the initial approximations of

$$\theta_{10}(r,z) = \frac{r^2 - h^2}{4} \text{ and } \sigma_{10}(r,z) = -\left(\frac{r^2 - h^2}{4}\right),$$

$$\theta_1 = (N_b - N_t)(N_b - 2N_t)\left(\frac{r^6 - h^6}{1152}\right) - (N_b - 2N_t)\left(\frac{r^4 - h^4}{64}\right), \tag{3.1}$$

$$\sigma_1 = -\left(\frac{N_t}{N_b}\right)(N_b - N_t)\left(\frac{r^4 - h^4}{64}\right). \tag{3.2}$$

Substituting Eq. (3.1) and Eq. (3.2) in Eq. (2.5) and applying boundary conditions Eq. (2.8) and Eq. (2.9), the expression for w is

$$w = -(1+\lambda_1)\frac{dp}{dz}\left(\frac{r^2}{4} - \frac{h^2}{4} - \frac{kh}{2}\right) + (1+\lambda_1)\frac{\sin\alpha}{F}\left(\frac{r^2}{4} - \frac{h^2}{4} - \frac{kh}{2}\right) + \frac{G_r}{1152}(1+\lambda_1)(N_b - N_t)(N_b - 2N_t)\left(\frac{r^8}{64} - \frac{r^2h^6}{4} + \frac{15h^8}{64} + \frac{3kh^7}{8}\right) - \frac{G_r}{64}(1+\lambda_1)(N_b - 2N_t)\left(\frac{r^6}{36} - \frac{r^2h^4}{4} + \frac{2h^6}{9} + \frac{kh^5}{3}\right) - \frac{B_r}{64}(1+\lambda_1)\left(\frac{N_t}{N_b}\right)(N_b - 2N_t)\left(\frac{r^6}{36} - \frac{r^2h^4}{4} + \frac{2h^6}{9} + \frac{k5^5}{3}\right). \tag{3.3}$$

In the moving frame, the dimensionless flux q is given by

$$q = \int_0^h 2rw\, dr. \tag{3.4}$$

The pressure drops over a wave length Δp_λ is calculated as follows:

$$\Delta p_\lambda = -\int_0^1 \frac{dp}{dz}\, dz. \tag{3.5}$$

The expression for Δp_λ is as follows

$$\Delta p_\lambda = qL_1 + L_2, \tag{3.6}$$

where

$$L_1 = -\frac{1}{1+\lambda_1}\int_0^1 \frac{1}{A}\, dz,$$

$$L_2 = -\frac{\sin\alpha}{F} + \frac{G_r}{576}(N_b - N_t)(N_b - 2N_t)\int_0^1 \frac{B}{A}\,dz - \frac{G_r}{32}(N_b - 2N_t)\int_0^1 \frac{C}{A}\,dz - \frac{B_r}{32}\left(\frac{N_t}{N_b}\right)(N_b - 2N_t)\int_0^1 \frac{C}{A}\,dz,$$

where,

$$A = \frac{h^4}{8} + \frac{kh^3}{2},$$

$$B = \frac{9h^{10}}{160} + \frac{3kh^9}{16},$$

$$C = \frac{5h^8}{96} + \frac{kh^7}{6}.$$

Using the same approach as Shapiro et al. [16], Over a period of time, the average time flux given by the laboratory frame was

$$\bar{Q} = 1 + \frac{\varepsilon^2}{2} + q. \qquad (3.7)$$

At the tube wall the dimensional less frictional force $\bar{F}$ is

$$\bar{F} = \int_0^1 h^2\left(-\frac{dp}{dz}\right)dz. \qquad (3.8)$$

The heat transfer coefficient and mass transfer coefficient at the tube wall are:

$$Z_\theta(r,z) = \left(\frac{\partial h}{\partial z}\right)\left(\frac{\partial \theta_1}{\partial r}\right)$$

and

$$Z_\sigma(r,z) = \left(\frac{\partial h}{\partial z}\right)\left(\frac{\partial \sigma_1}{\partial r}\right). \qquad (3.9)$$

4. Findings and Discussions

The graphs depicting axial velocity, pressure drop, frictional force, heat transfer coefficient, and mass transfer coefficient were developed using Mathematica 11.0 software.

4.1 Pressure Drop

Figs. 1-7 plots the pressure drop versus time averaged flux for various values of flow parameters. It is observed that, increasing in N_b, λ_1, α, there is a negative impact in pressure drop. This has therapeutic implications since sustaining larger pressure gradients, which has a demonstrable influence in the drug delivery system, has implications. Δp_λ increases for greater magnitude of thermophoresis N_t, G_r, B_r and k.

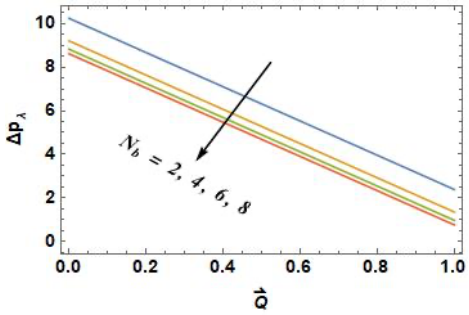

Fig. 1. Fluctuations in Pressure Drop for N_b.

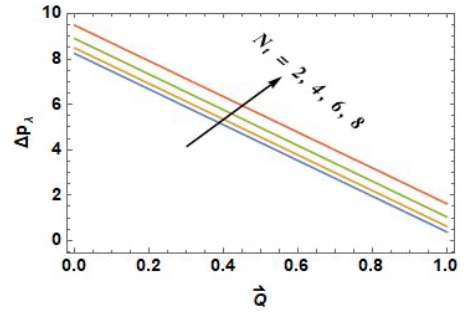

Fig. 2. Fluctuations in Pressure Drop for N_t.

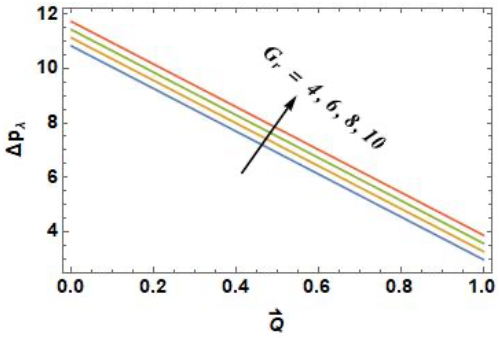

Fig. 3. Fluctuations in Pressure Drop for G_r.

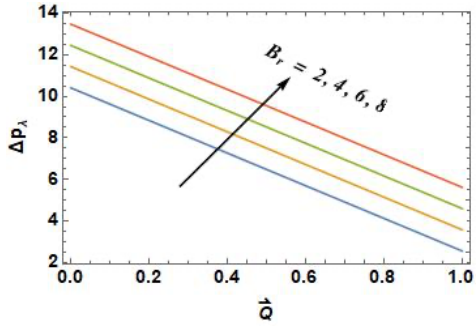

Fig. 4. Fluctuations in Pressure Drop for B_r.

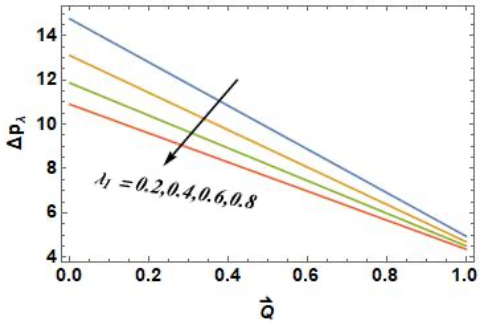

Fig. 5. Fluctuations in Pressure Drop for λ_1.

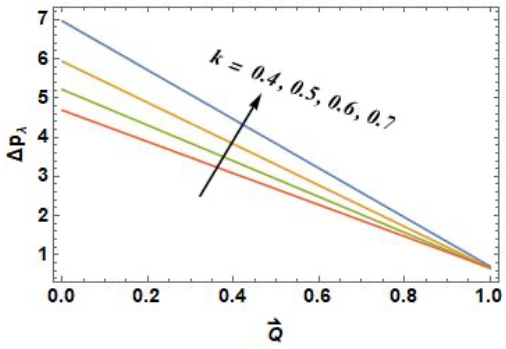

Fig. 6. Fluctuations in Pressure Drop for k.

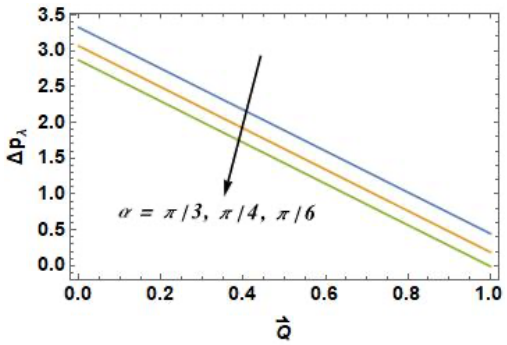

Fig. 7. Fluctuations in Pressure Drop for α.

4.2 Frictional force

It is apparent that, frictional forces $\bar{F}$ is upsurged by growing N_t, G_r, B_r, α.

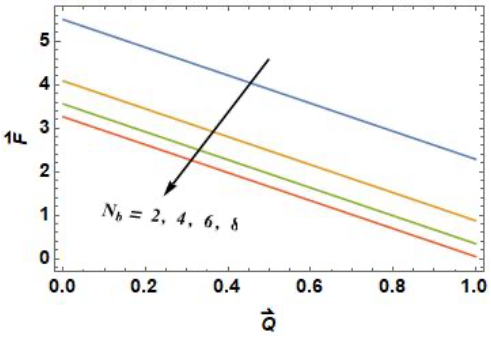

Fig. 8. Fluctuations in Frictional Force for N_b.

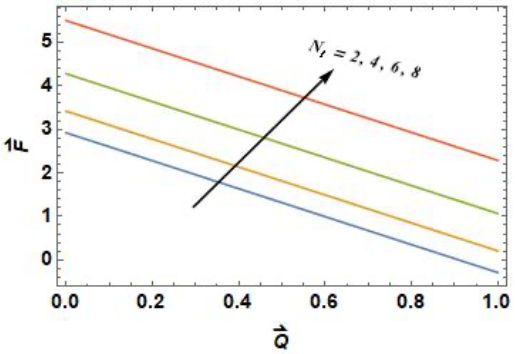

Fig. 9. Fluctuations in Frictional Force for N_t.

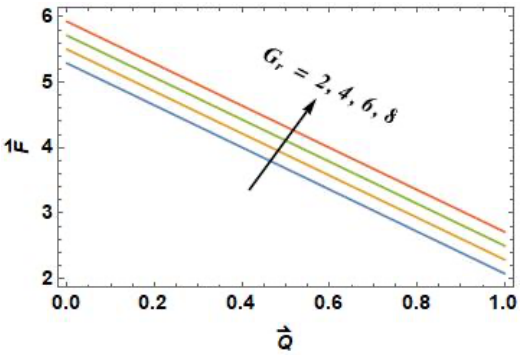

Fig. 10. Fluctuations in Frictional Force for G_r.

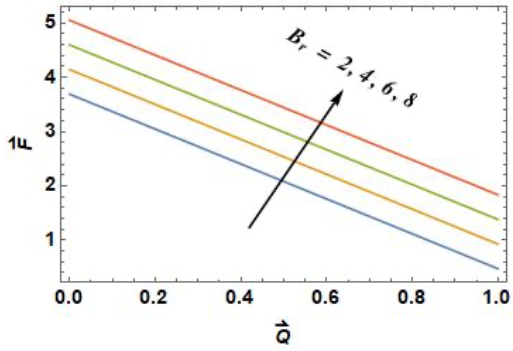

Fig. 11. Fluctuations in Frictional Force for B_r.

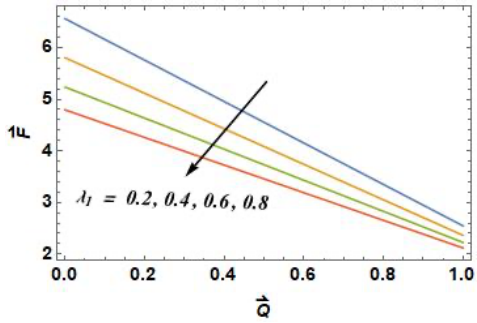

Fig. 12. Fluctuations in Frictional Force for λ_1.

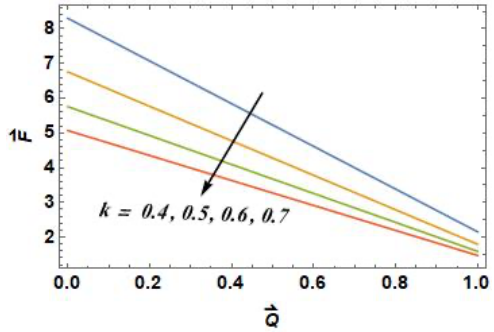

Fig. 13. Fluctuations in Frictional Force for k.

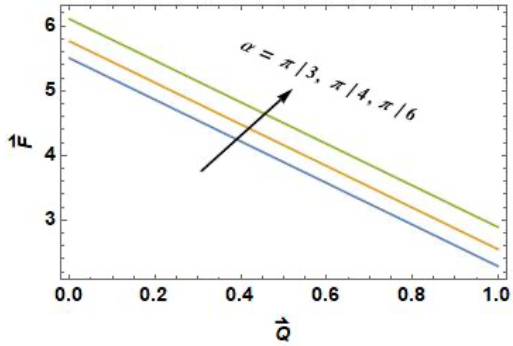

Fig. 14. Fluctuations in Frictional Force for α.

4.3 Temperature

Significant raise in temperature is sustained as the upsurges in Brownian motion (N_b) and an opposite behaviour is found with thermophoresis.

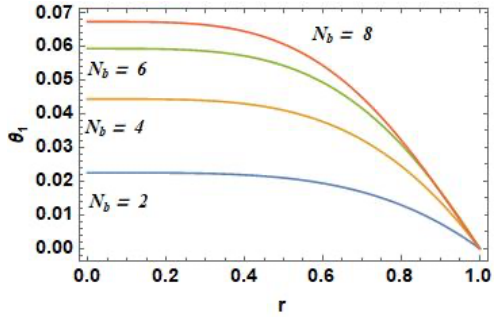

Fig. 15. Effect of N_b on Temperature.

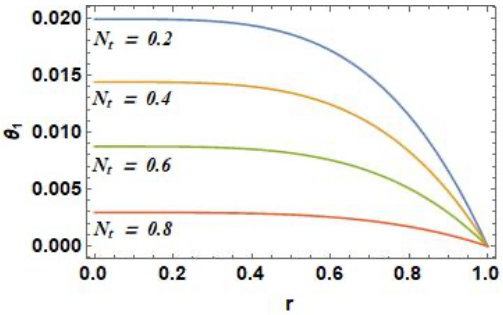

Fig. 16. Effect of N_t on Temperature.

4.4 Concentration

It can be seen from the graph that concentration increases as N_t increases. It may be deduced that a constant increase in the firmness of thermophoretic effects results in a larger mass flow as temperature rises, increasing the concentration.

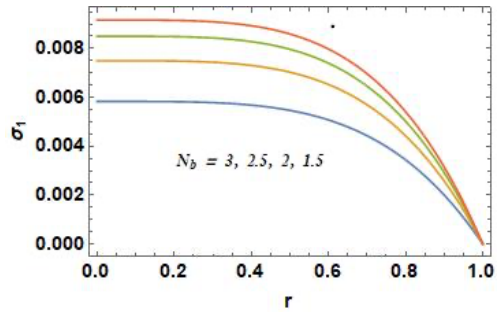

Fig. 17. Effect of N_b on Concentration.

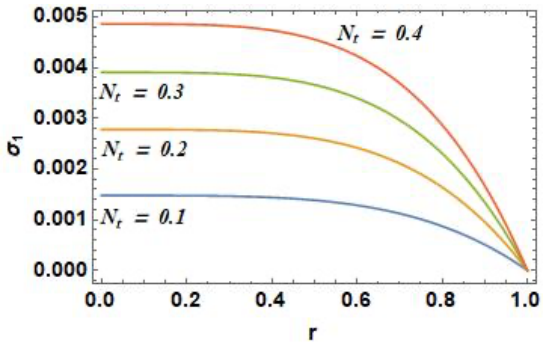

Fig. 18. Effect of N_t on Concentration.

4.5 Heat Transfer Coefficient

It is interesting to observe that, absolute value of coefficient of heat transfer is increasing for N_b and decreasing for N_t.

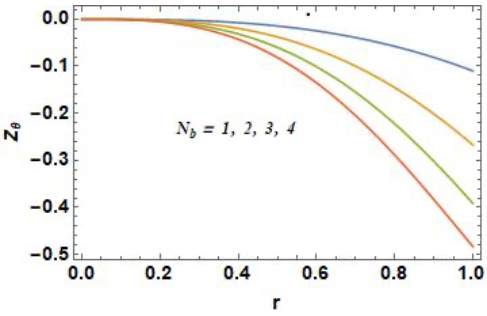

Fig. 19. Impact of N_b on Heat Transfer Coefficient.

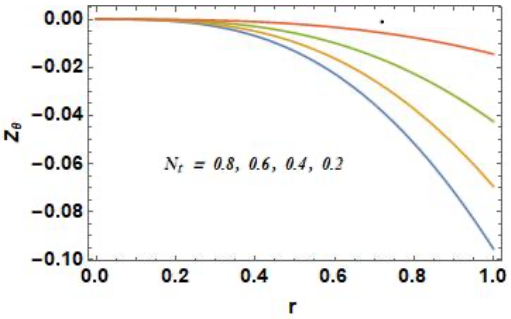

Fig. 20. Impact of N_t on Heat Transfer Coefficient.

4.6 Mass Transfer Coefficient

It is observed that, absolute value of coefficient of mass transfer is increasing for N_b and decreasing for N_t.

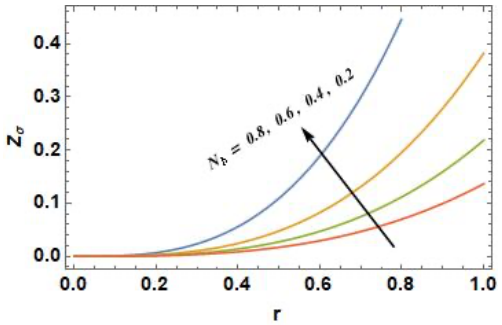

Fig. 21. Impact of N_b on Mass Transfer Coefficient.

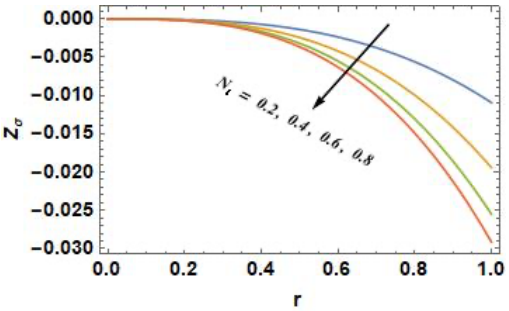

Fig. 22. Impact of N_t on Mass Transfer Coefficient.

4.7 Trapping

In peristaltic motion, the trapping phenomena is much more thought-provoking. The following figures shows that, the size of the trapped bolus increases with the increases of parameters. So physically the velocity can be controlled by increasing/decreasing these pertinent parameters.

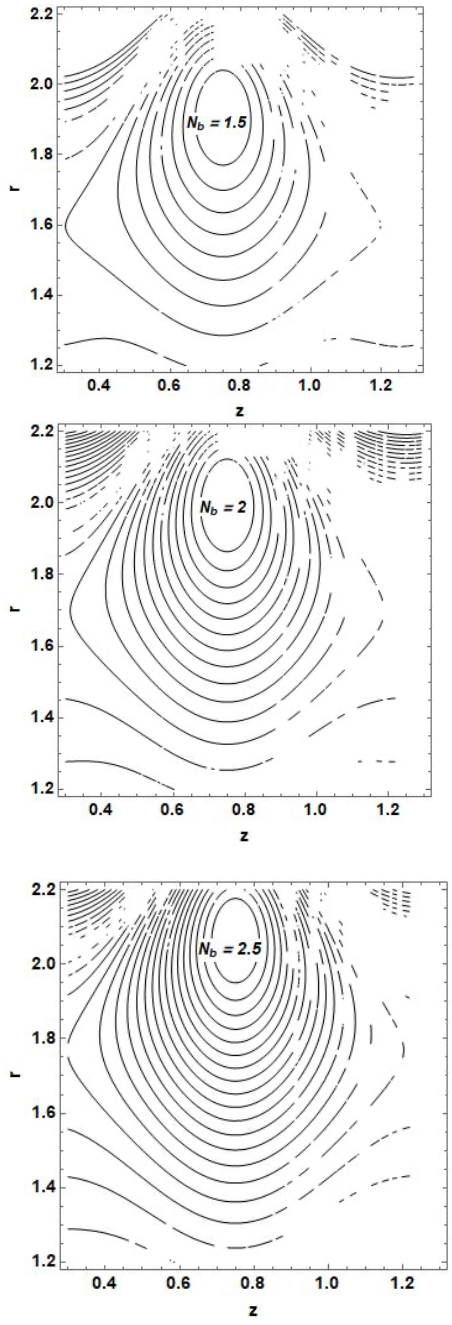

Fig. 23. Streamlines for different values of N_b.

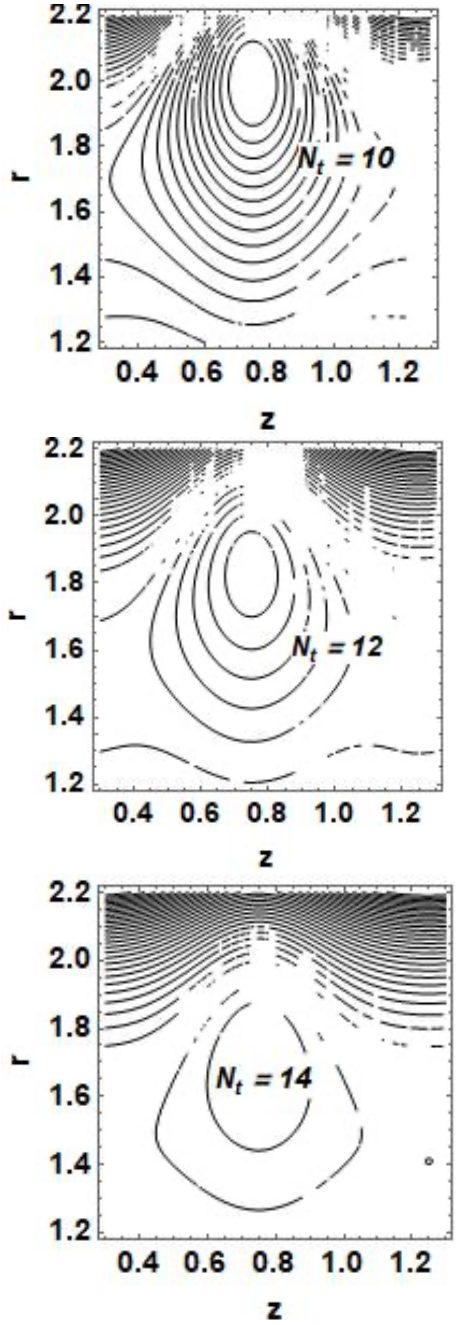

Fig. 24. Streamlines for different values of N_t.

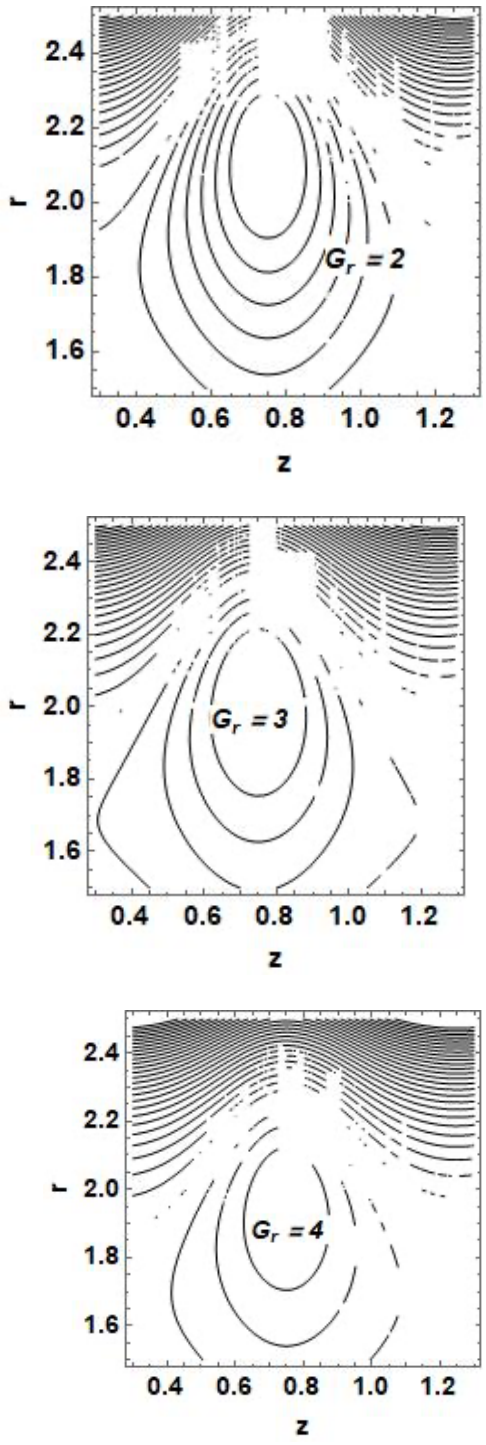

Fig. 25. Streamlines for different values of G_r.

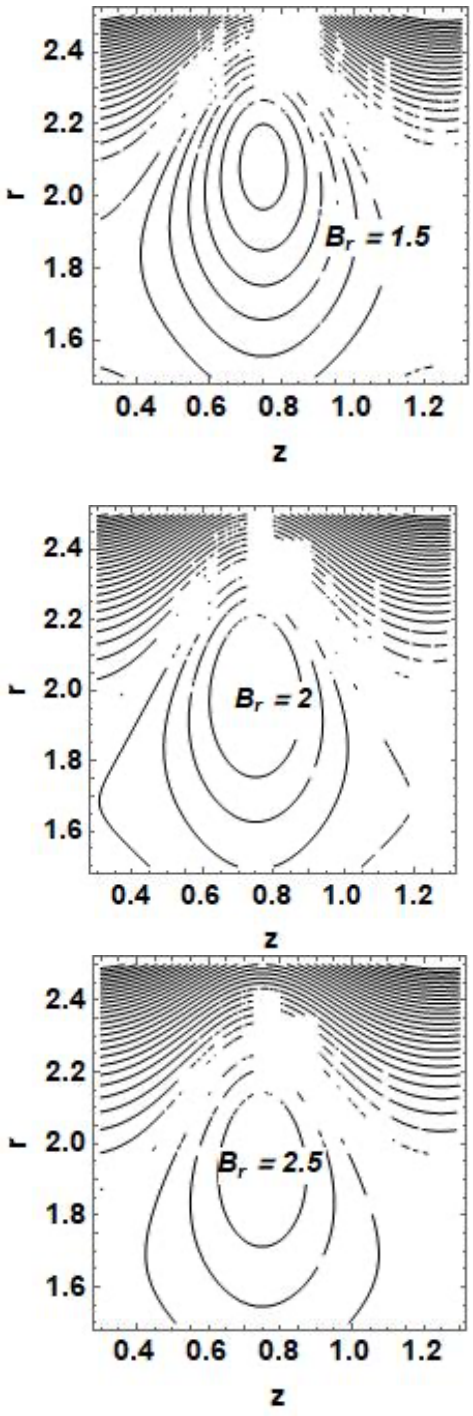

Fig. 26. Streamlines for different values of B_r.

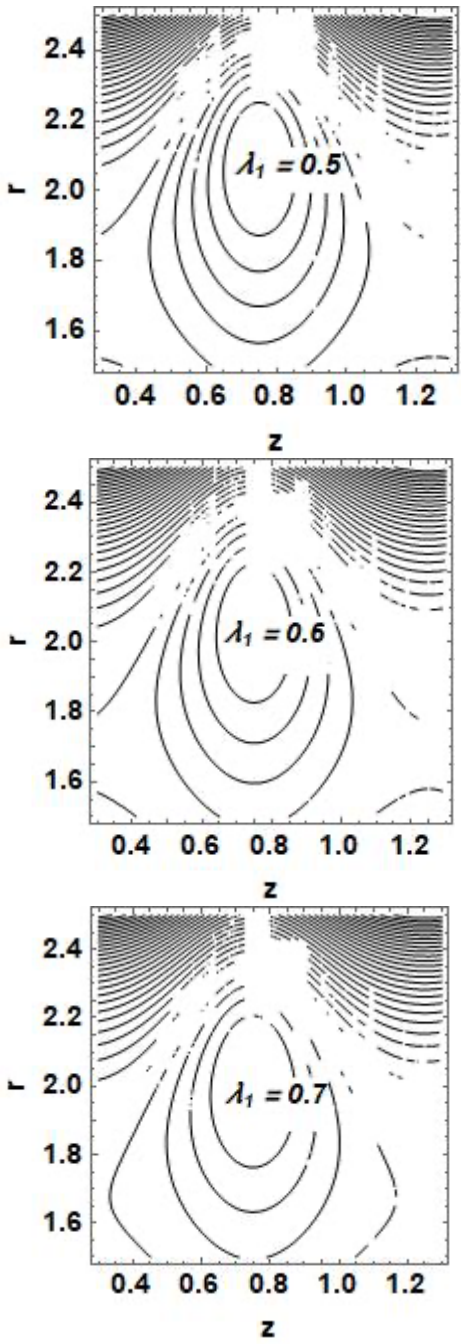

Fig. 27. Streamlines for different values of λ_1.

The results of this paper are coinciding with results of the paper of Subhadra et al. if no slip boundary condition is used in a straight tube.

5. Conclusion

(i) The major conclusions of this investigations are

(ii) If there is an increase in N_b, λ_1, α, there is a negative impact on pressure drop.

(iii) Frictional force $\bar{F}$ is upsurged by growing N_t, G_r, B_r, α.

(iv) Significant raise in temperature is sustained as the upsurges in Brownian motion (N_b) and an opposite behaviour is found with thermophoresis.

(v) Concentration increases as N_t increases. It may be deduced that a constant increase in the firmness of thermophoretic effects results in a larger mass flow as temperature rises, increasing the concentration.

(vi) Absolute value of coefficient of heat transfer is increasing for N_b and decreasing for N_t.

(vii) Absolute value of coefficient of mass transfer is increasing for N_b and decreasing for N_t.

(viii) The size of the trapped bolus increases with the increases of parameters. So physically the velocity can be controlled by increasing/decreasing these pertinent parameters.

References

[1] Shapiro, A.H., Jaffrin, M.Y., Weinberg, S.L., (1969). Peristaltic pumping with long wavelengths at low Reynolds number. J. Fluid Mech. 37, 799-825.

[2] Chu, W.K.-H., Fang, J., (2000). Peristaltic transport in a slip flow. Eur. Phys. J. B- Condens. Matter Complex Syst. 16, 543-7.

[3] Maruthi Prasad, K., Radhakrishnamacharya, G., (2008). Flow of Herschel–Bulkley fluid through an inclined tube of non-uniform cross-

section with multiple stenoses. Arch. Mech. 60, 161-72.

[4] Prasad, K.M., Subadra, N., Srinivas, M., (2017). Thermal Effects of Two Immiscible Fluids in a Circular Tube with Nano Particles. J. Nanofluids 6, 105-19.

[5] N. Subadra, M. A. Srinivas, and Sunil Dutt Purohit, (2020). Mathematical approach to study heat and mass transfer effects in transport phenomena of a non-Newtonian fluid, AIP Conference Proceedings 2269, 060006.

[6] S. U.S. Choi, J.A.E., (1995). Enhancing thermal conductivity of fluids with nanoparticles. ASME FED. Proc. ASME Int. Mech. Eng. Congr. Expo. 66.https://doi.org/10.3390/app8020192

[7] Eastman, J., Choi, U., Li, S., Thompson, L., Lee, S., (1996). Enhanced thermal conductivity through the development of nanofluids. Presented at the MRS proceedings, Cambridge Univ Press, p. 3.

[8] K Maruthi Prasad, N Subadra. (2019). Influence of Slip-on Peristaltic Motion of a Nanofluid Prone to the Tube, Numerical Heat Transfer and Fluid Flow, 519-26.

[9] Ellahi, R., (2018). Special Issue on Recent Developments of Nanofluids. Appl. Sci. 8, 192.

[10] Agrawal, P., Dadheech, P. K., Jat, R. N., Nisar, K. S., Bohra, M., & Purohit, S. D., (2021). Magneto Marangoni flow of γ− AL2O3 nanofluids with thermal radiation and heat source/sink effects over a stretching surface embedded in porous medium. Case Studies in Thermal Engineering, 23, 100802., https://doi.org/10.1016/j.csite.2020.100802

[11] Jamshed, W., Nasir, N.A.A.M., Isa, S.S.P.M. et al., (2021). Thermal Growth in Solar Water Pump using Prandtl–Eyring Hybrid Nanofluid: A Solar Energy Application. Scientific Reports, 11, 18704. https://doi.org/10.1038/s41598-021-98103-8

[12] W. Jamshed, Kottakkaran Sooppy Nisar, (2021). Computational Single Phase Comparative Study of Williamson Nanofluid in Parabolic Trough Solar Collector Via Keller box Method, International Journal of Energy Research, https://doi.org/10.1002/er.6554

[13] Naby, A. E. H. A. El, & Shamy, I. El. (2007). Slip effects on peristaltic transport of power-law fluid through an inclined tube. Applied Mathematical Sciences, 1(60), 2967-80.

[14] Hayat, T., Abbasi, F. M., Ahmad, B., & Alsaedi, A. (2014). Peristaltic transport of Carreau-Yasuda fluid in a curved channel with slip effects. PloS One, 9(4), e95070.

[15] Nadeem, S., Riaz, A., Ellahi, R., Akbar, N.S., (2014). Mathematical model for the peristaltic flow of Jeffrey fluid with nanoparticles phenomenon through a rectangular duct. Appl. Nanosci. 4, 613–624. https://doi.org/10.1007/s13204-013-0238-5

[16] He JH. (1999). Homotopy Perturbation Technique. Comput. Methods Appl. Mech. Eng. 178, 257-62.

[17] N Subadra, K Maruthi Prasad, S Ravi Prasad Rao, (2020), Influence of Slip and Heat and Mass Transfer Effects on Peristaltic motion of Power-law fluid Prone to the Tube, Journal of Physics: Conference Series, 1495(1), 012039.